Universiteit Antwerpen

Calibration of physical transport in a 1D estuarine ecosystem model, based on tracer output from a 3D hydrodynamic model

Calibration, verification and steady-state simulations

dr. Tom Van Engeland
dr. ir. Tom J.S. Cox
dr. ir. Stefan Van Damme
prof. dr. Patrick Meire

Report number ECOBE 015-R187

September 2015

Colophon

Report research group Ecosystem Management ECOBE 015-R187

This report should cited as:

Van Engeland, T. ; Cox, T.; Van Damme S. ; Meire, P. (2015) Calibration of physical transport in a 1D estuarine ecosystem model, based on tracer output from a 3D hydrodynamic model. Calibration, verification, and steady-state simulations.. University Antwerp, Ecosystem Management research group, ECOBE 015-R187

University of Antwerp "Campus Drie Eiken"
Prof. dr. P. Meire
Departement of Biologie
Ecosystem Management research group
Universiteitsplein 1
BE-2610 Antwerpen (Wilrijk)
Tel.+32 3 820 22 68
Fax+32 3 820 22 71
e-mail: Patrick.Meire@uantwerpen.be
http://www.ua.ac.be/ecobe

Table of Contents

1. Introduction

For the project 13_131 “integrated plan Upper Sea Scheldt, the University of Antwerp (UA) , Flanders Hydraulics Research (FHR) and the Research Institute for Nature and Forestry (RINF) are involved in a joint modeling effort with a 3D hydrodynamic model (FHR), a 1D biogeochemical/ecosystem model with simplified reactive transport (UA), and a set of statistical models focusing on higher trophic levels of the food web (INBO). Information on effects of management decisions in the Upper Sea Scheldt flows mainly from lower to higher organizational levels, starting with detailed hydrodynamics and sediment transport (FHR), over biogeochemistry and primary production (UA), to habitat characteristics and effects on key species (INBO). For more details we refer to document *IMDC/INBO/UA/WL (2014)*.

However, there is also an information flow from the 1D ecosystem model to the sediment transport model. Fine sediment transport is dependent on the salinity field. Due to the high computational costs, generating a stable salinity field with the 3D hydrodynamic model is not feasible within the current time constraints. To overcome this problem an additional iteration between the 3D hydrodynamic model and the 1D ecosystem model was devised. The simplified volumetric transport from the 1D model is sufficient to generate an initial salinity gradient for the simulations of 3D model, provided that this transport is realistically parameterized.

This document reports on the initial calibrations of the dispersion coefficients in the 1D model based on tracer output from the 3D hydrodynamic model, and the generation of a steady-state salinity gradient that will serve as initial condition for the longer simulations of the various alternatives with the 3D model. Although it is questionable whether the salinity field in the Schelde estuary ever reaches a stable state, it could serve as a best guess for an initial state in the 3D hydrodynamic model.

This report is limited to the reference simulation for 2013.

2. Deliverables

The output from the transport component of the 1D model consists of a set of salinity concentrations as function of distance from the upstream boundary near Ghent. This salinity gradient is conditional on the discharge values imposed at the boundaries Upper Scheldt, Dender, Rupel, Bathse Spui, and the canal Ghent-Terneuzen. These discharges are provided along with the salinity gradient.

3. Approach

The transport component of the 1D ecosystem model was tuned to the transport as resolved by the 3D hydrodynamic model by calibration to concentrations of fictive passive tracer injected at the beginning of a simulation run with the 3D model. The following sections explain the steps taken in data processing, calibration and generation of the salinity gradient.

3.1 Data delivery and processing

Tracer concentrations, discharge values, and morphological information per time step (1 hour) and per 1D model segment were provided by FHR as detailed in WL2015_131_12 (2015). Figure 1 shows the tracer distribution 13 hours into the simulation run of the 3D model (A) and the applied discharge signals at the boundaries (B).

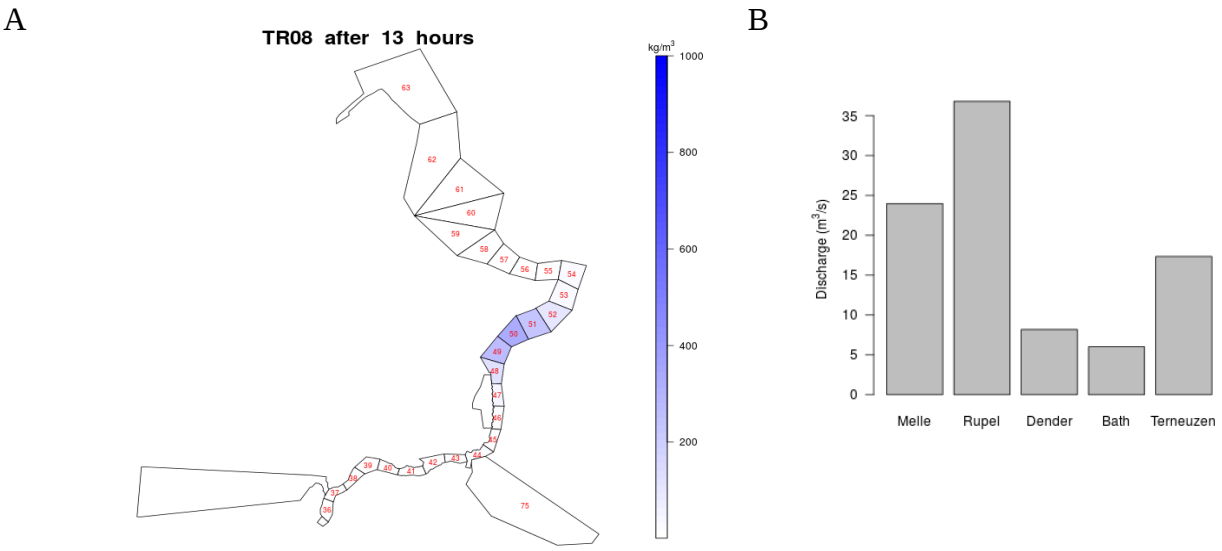

Figure 1: Tracer data from the 3D hydrodynamic model (A) 13 hours after injection into box 48, and the constant discharge values that were used during these simulations (B).

Due to the high sensitivity of the model fit to small mismatches in timing between model output and data, it was decided to remove the tidal signal from the tracer data (Fig. 2). This was accomplished by tracking the tracer maxima over time, and shifting the series accordingly. The day-to-day trend in the tracer movement, resulting from discharge, was estimated using a spline smoother (Fig. 2 upper graph). The difference between this spline smoother and the actual signal was used to shift the series, such that only a trend (average lateral transport) remained. We acknowledge that this may introduce some uncertainty, because the dispersive effects of a box in the far range of a tidal excursion relative to a specific box is shifted towards that box. However, because of the spatial dependence in dispersive properties between neighboring boxes the adverse effects are negligible. In addition to the removal of the tidal signal, the volumes of the active CRT systems were added to the connecting model boxes, and tracer concentrations were recalculated to preserve the mass balance.

3.2 Calibration of dispersive transport

The volumetric transport in the 1D ecosystem model consists of a unidirectional advective component and a diffusive/dispersive component (first and second term respectively), and is based on equation (3.16) in Soetaert and Herman (2009):

$$\frac{\delta C}{\delta t} = -\frac{1}{A} \cdot \frac{\delta (Q.C)}{\delta x} + \frac{1}{A} \cdot \left(A.D \frac{\delta C}{\delta x} \right) + reaction$$

with C the tracer concentration, A the surface area of the box interfaces, Q the discharge, and D a dispersion coefficient. If this formula is discretized for a series of boxes, and we assume that

$$V_i = A_i \cdot x_i$$

the formula becomes:

$$\frac{dC_i}{dt} = -\frac{\Delta_i (Q.C)}{\Delta V_i} + \frac{\left(A_i . D_i \frac{\Delta C_i}{\Delta x_i} \right)}{V_i} + reac_i$$

The only free parameter in this transport model is the dispersion parameter D, which can either be kept constant over the model segments or is allowed to vary per box edge (D_i rather than D). In this calibration exercise it is allowed to vary per box, since it is well established that one dispersion parameter for the entire estuary is not optimal to reproduce a realistic salinity gradient (pers. comm. Joris Vanlede). Therefore, a subset of the 77 possible dispersion coefficients were fitted with optimization routines, while the remainder was determined through linear interpolation between these selected parameters. Dispersion at the upstream boundaries was assumed to be zero.

Apart from the calibration on tracer data from the 3D model, a second trajectory was followed with calibration on chloride-based salinity data. For this salinity-based calibration, salinity and discharge data from 2010 until 2012 were used. A subset of dispersion coefficients was first adjusted manually to obtain a first guess for the optimization routines. This manual fit was performed on the tracer and salinity data together. The resulting parameter set was subsequently used for an automatic calibrations on salinity and on tracer data separately. Automatic calibrations consisted of an initial optimization with a Levenberg-Marquardt algorithm, followed by a series of Markov-Chain Monte-Carlo simulations (MCMC; Delayed-Rejection Adaptive Metropolis-Hastings algorithm) to explore the stability of the solution. The applied cost function used a simple least-squares approach.

3.3 Generation of an initial salinity field for the 3D model

Using the estimated dispersion parameter set, the 1D transport model was run to steady-state, under a constant discharge, to obtain a stable salinity gradient. This salinity gradient was compared to monitoring data (OMES, MWTL) with similar discharge conditions. The discharge values were taken from the planned model simulations of the 3D model.

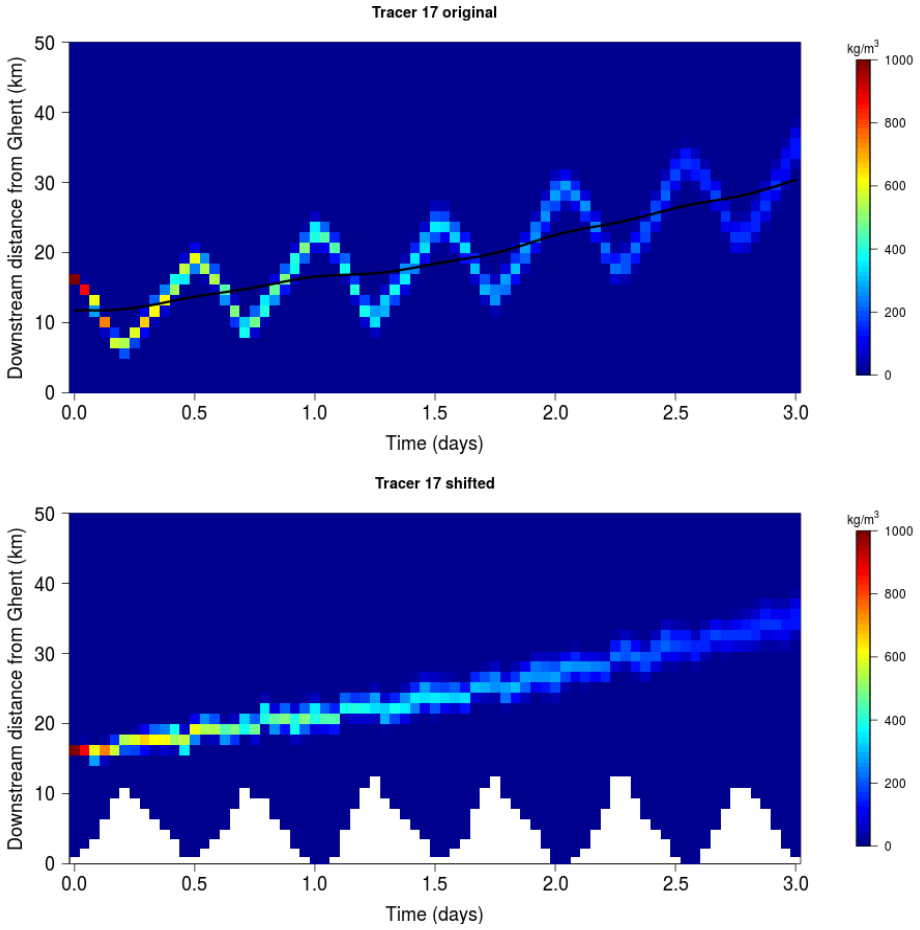

Figure 2: Tracer evolution of time and space as provided by 3D hydrodynamic model (upper), and a shifted version without tidal variability (lower). The smooth spline in the upper graph represents the estimated lateral transport, based on the concentration maxima.

4. Results

4.1 Model calibration

The dispersion coefficients were mainly selected from the lower Seascheldt where the salinity gradient is strongest. Figures 3 to 6 show the results from the final MCMC calibration on tracer data and on salinity data.

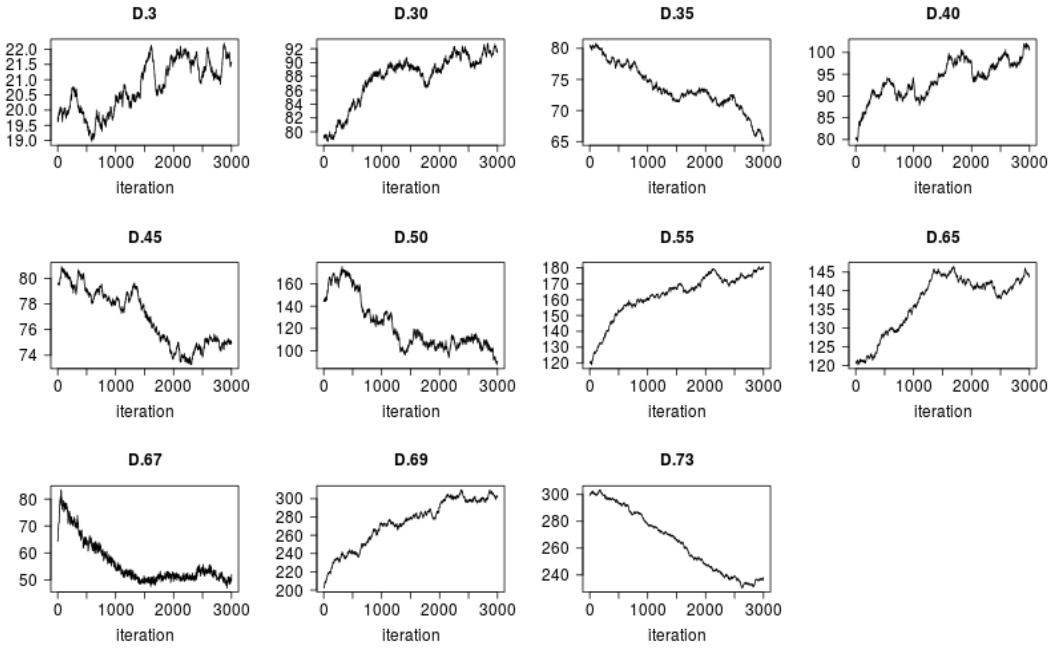

*Figure 3: Trace of the final Markov-Chain Monte-Carlo calibration on **salinity**. The position of these dispersion coefficients is indicated above each graph by the index (starting with 1 near Ghent). Dispersion at the upstream boundaries of the main axis and the river Rupel are forced to 0 m^2/s (no dispersive exchange).*

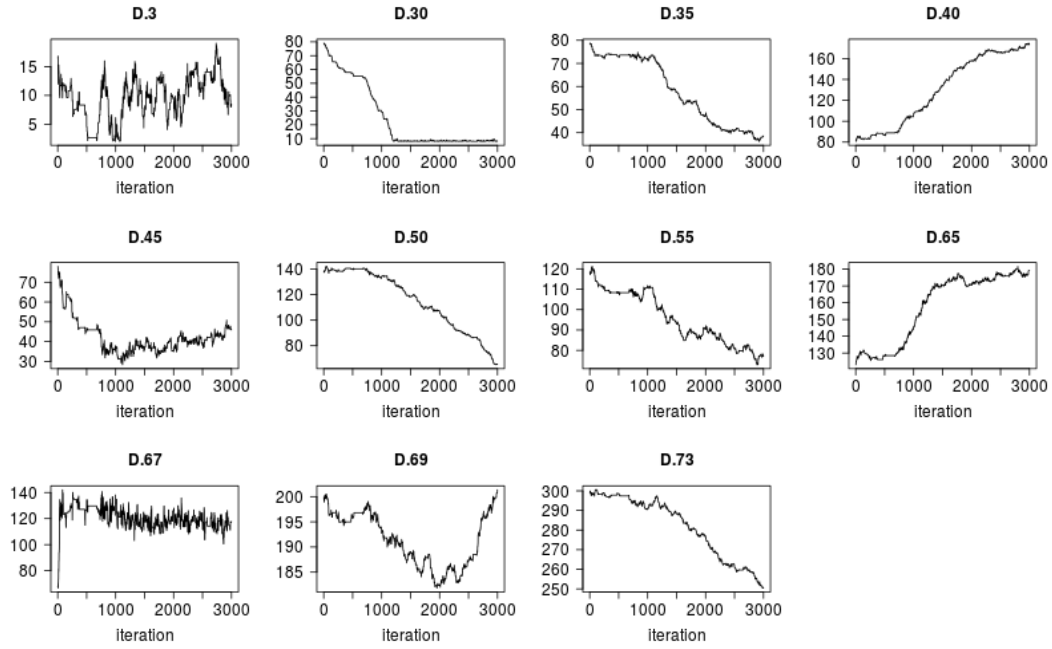

*Figure 4: Trace of the final Markov-Chain Monte-Carlo calibration on **tracer data**. The position of these dispersion coefficients is indicated above each graph by the index (starting with 1 near Ghent). Dispersion at the upstream boundary of the main axis and the river Rupel are forced to 0 m^2/s (no dispersive exchange).*

After systematic removal of a number of dispersion coefficients from the initial parameter set, the final parameter set consisted of 10 dispersion coefficients spread out over the salinity gradient, and one coefficient upstream. Further removal of parameters resulted in poorer fitting results. However, from the trends in the traces of the final MCMC simulations (Fig. 3 and 4) it is clear that these algorithms did not converge to a final single parameter set (even after a total of 20000 iterations), but rather kept "wondering" through parameter space. This apparent over-parameterization is reflected in stronger correlations between estimated dispersion coefficients (Figs. 5 and 6), which could be expected for neighboring coefficients, but not necessarily for pairs at greater distances. After removal of D.35 and D.55 model fidelity to salinity data deteriorated (data not shown). Over-parameterization was expected for the calibration on salinity, but not on the tracer simulations, since in the latter case more variables were available with strong local variability (and therefore higher expected information content).

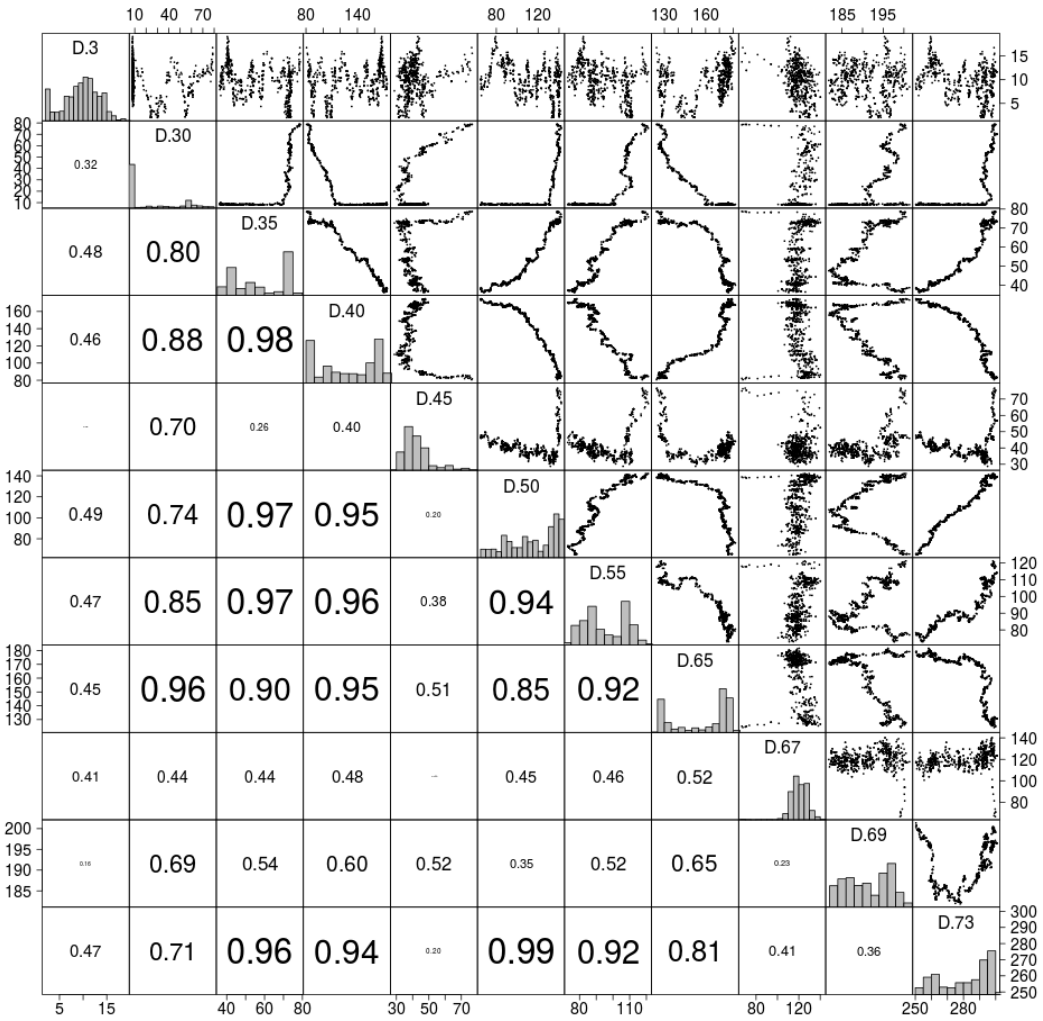

Figure 5: Scatterplot (upper triangle), distributions (diagonal) and linear correlation coefficients (lower triangle) of a random subset of dispersion coefficient combinations that were accepted by the Markov-Chain Monte-Carlo simulation.

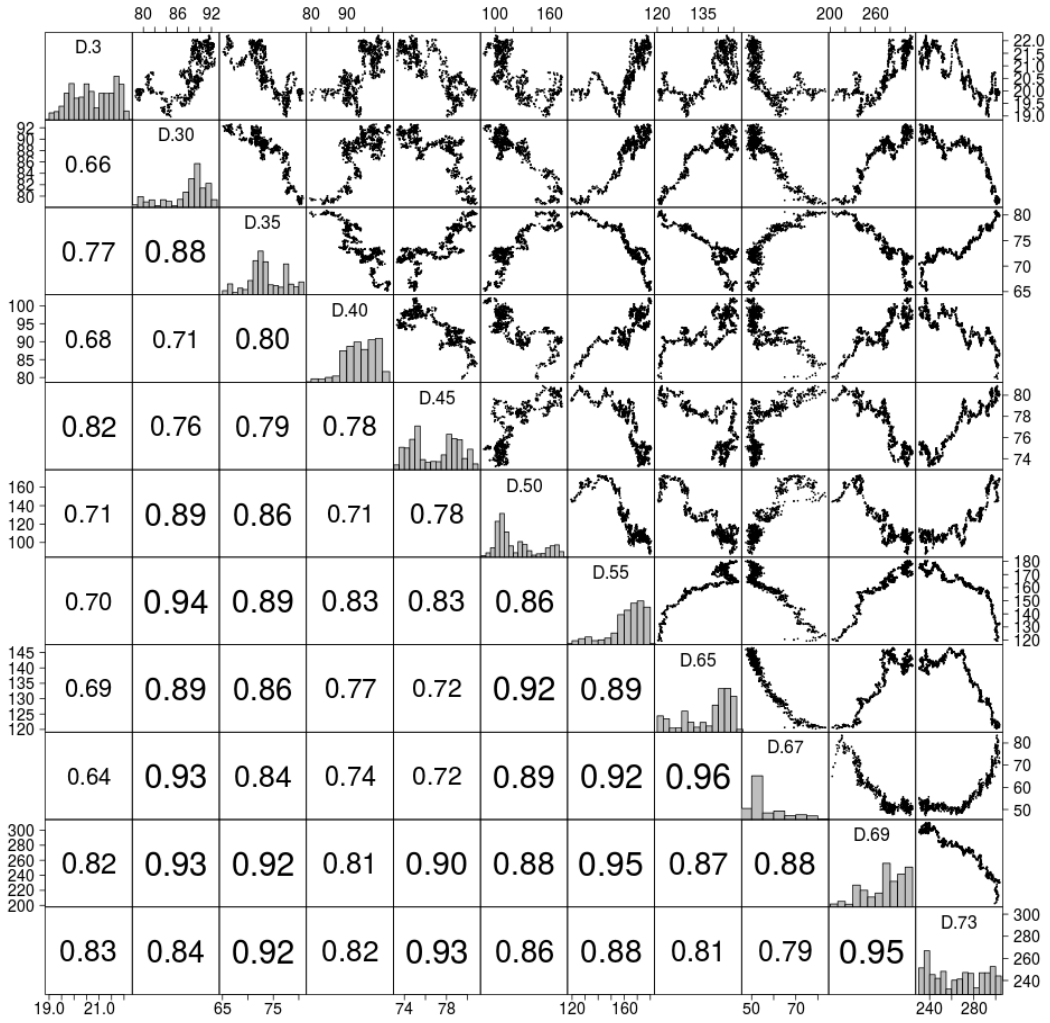

Figure 6: Scatterplot (upper triangle), distributions (diagonal) and linear correlation coefficients (lower triangle) of a random subset of dispersion coefficient combinations that were accepted by the Markov-Chain Monte-Carlo simulation.

The resulting parameter uncertainty for the respective calibration exercises is shown in figure 7. The overall longitudinal trend is similar for both parameter sets, but slightly stronger dispersive behavior is suggested in the Upper Seascheldt by the salinity-based calibration. The drop in dispersive transport around 120 km from Ghent (near Saeftinghe) is consistent in for both parameter sets but more pronounced in the set calibrated with salinity.

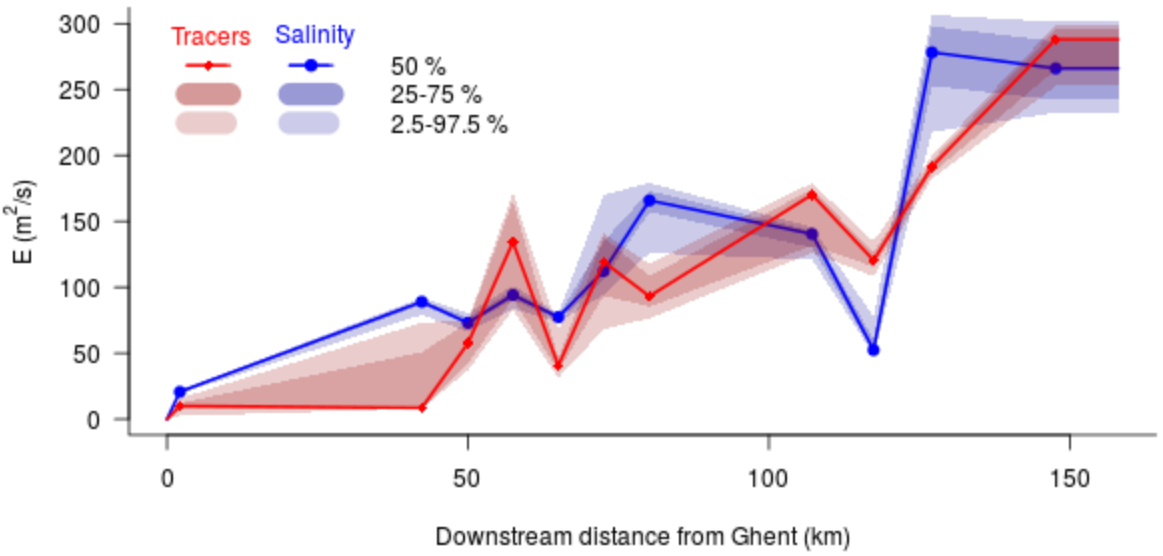

Figure 7: Variability in the dispersion coefficients from the tracer-based (red) and salinity-based calibration (blue). The breakpoints of these curves are the dispersion coefficients that were actually fitted to the tracer data. The 95% estimation intervals are indicated as light colored regions, the inter-quartile ranges as darker regions. The median values are indicated as solid lines.

4.2. Model verification

The estimates from the two calibration exercises were compared to data from MWTL (Dutch) and OMES (Flemish) monitoring for the years 2010 – 2012. Model output at steady state was compared to a subset of data with similar discharge regimes (Fig. 8), whereas all data were used to compare the dynamic model run (Fig. 9). Boundary and initial conditions were chosen from the same time period.

Despite the fact that the fitting problem was underdetermined, model output uncertainty was acceptable for both parameter sets. Both steady-state profiles fell within the range of observed variability (Fig. 8), and exhibited similar performance in generating a salinity gradient, although a distinction existed near the upstream part of the salinity gradient (50 – 80 km) and in the upper reaches of the Western Scheldt (100 – 120 km). The downward deviation in the overall trend near 100 km, suggested by the data, is visible in the salinity-based profile (blue), but much less pronounced in the tracer-based profile (red). In addition, the tracer-based profile showed a tendency towards the higher end of the salinity distribution in the lower Seascheldt.

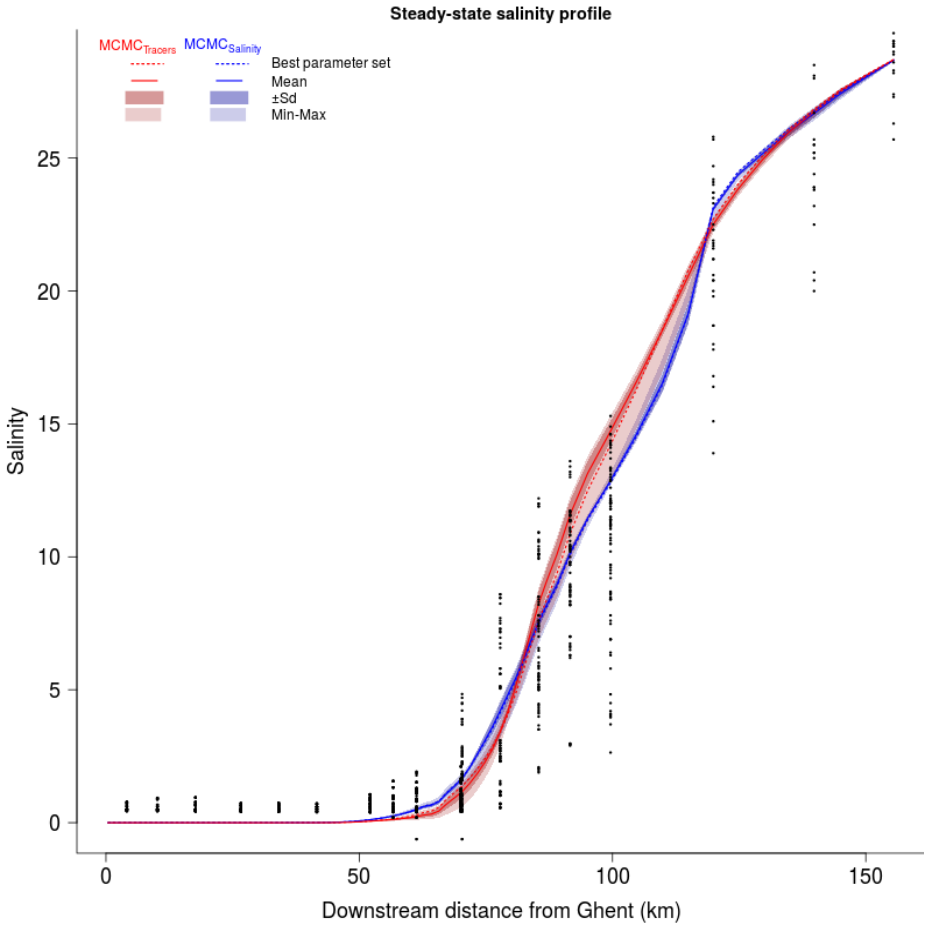

Figure 8: Steady-state salinity distribution along the estuarine axis. Tracer-based results are indicated in red, salinity-based results in blue. The dotted lines are model results from the manual fits. Observations (dots) are related to similar discharge conditions as those of the 3D model.

The dynamic model runs exhibited a fairly good agreement for the Western Scheldt (boxes 67 and 71 in figure 9), for the tracer- (red) as well as the salinity-based (blue) parameterization. Larger deviations occurred during periods of low salinity in the upstream part of the lower Seascheldt, and in the lower reaches of the Upper Seascheldt. Despite the apparent over-parameterization, it was not possible to "bend" the model towards these lower salinities without deviating in the higher salinities. Most likely this is related to deviances in discharge, particularly in the Rupel, where it is not measured directly. This is supported by the location of the deviations in salinity downstream of the Rupel mouth (box 44). Both parameter sets performed similarly in this respect.

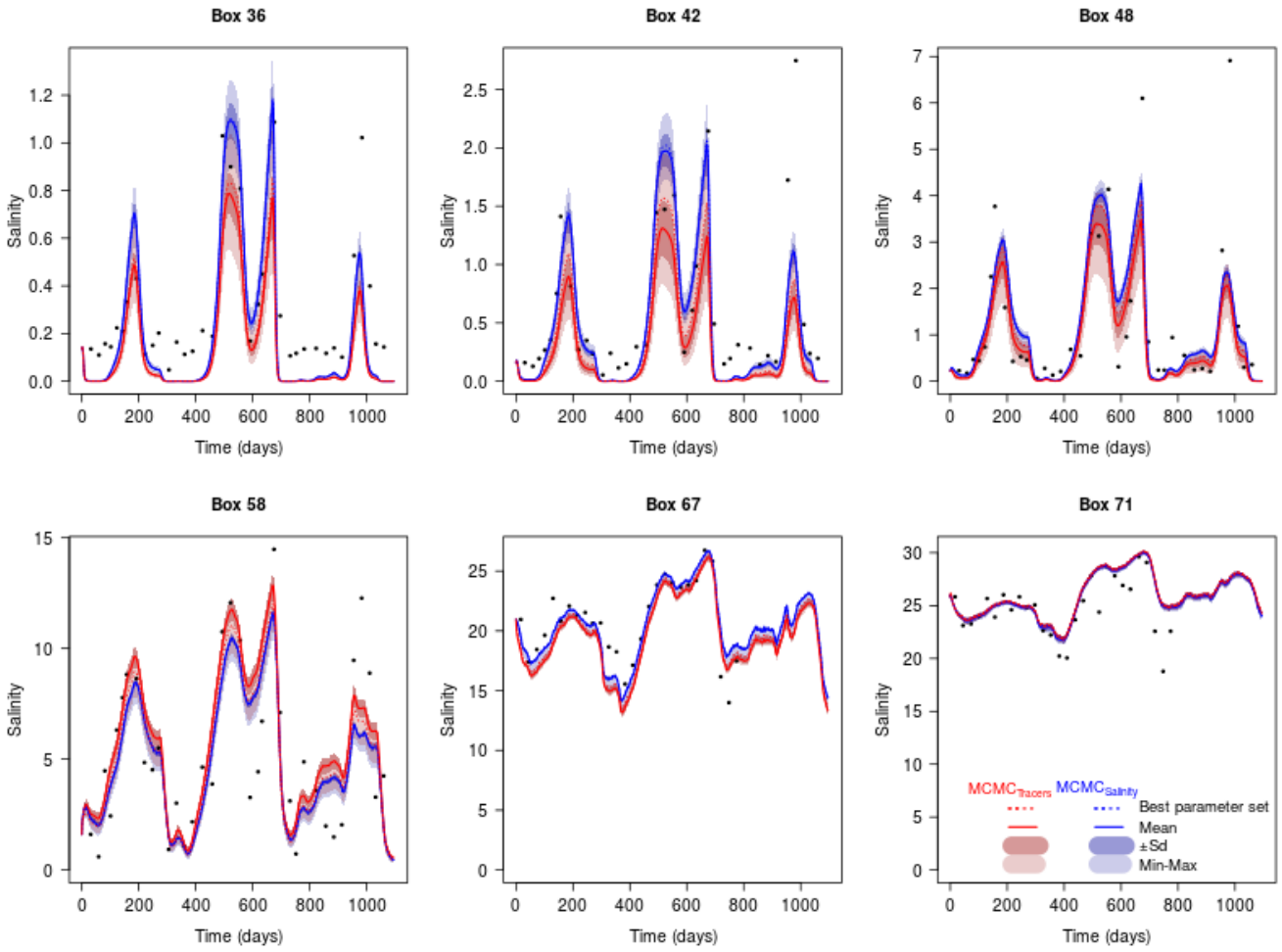

Figure 9: Dynamic model runs with tracer- and salinity-derived dispersion coefficients. Color codes are the same as for figure 8. The model boxes are indicated on top of each graph (see Fig. 1 for their location).

4.3 Steady-state salinity profiles for 3D initial conditions

The 3D hydrodynamic model needs a stable salinity gradient as starting condition to avoid costly model spin-up time, while retaining independence of the simulation from its initial state. For this purpose, steady-state salinity gradients were simulated with our 1D transport sub-model, while assuming the initial discharge conditions as planned for the 3D model simulations. The average salinity near Vlissingen in 2013 was chosen as salinity on the downstream boundary of our model domain. The model was run to steady-state over 2500 days, but had already converged to a large extent after 250 days (Fig. 10). The profiles after 2500 days are provided the FHR for the simulation of the 2013 reference situation.

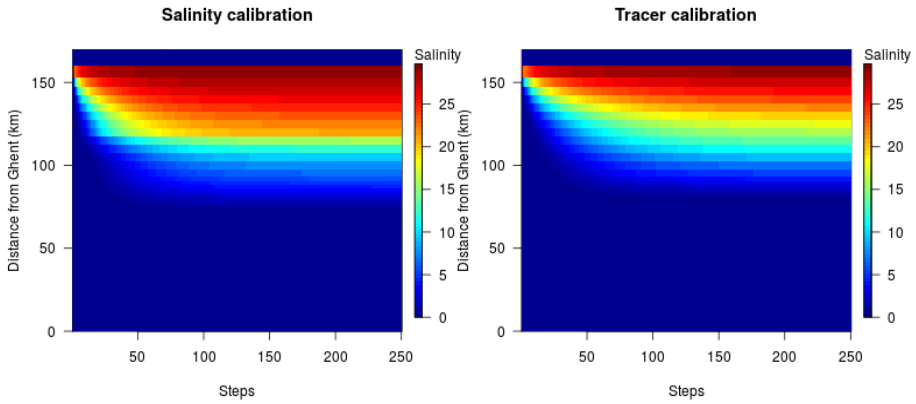

Figure 10: Model simulations evolving to a steady state in the first 250 of 2500 steps.

5. Final remarks

So far, this report seems to suggest that over-parameterization may be problematic when one is interested in the parameter values, but not necessarily when only the model output is relevant. This is, however, not true. Earlier calibration runs have shown that a good fit to the tracer data does not necessarily provide a realistic salinity field. The model-data comparison in figure 11 is based on one of the first calibration runs, where a slightly different strategy was followed. Rather than starting from the same manually fitted initial parameter set, separate manual fits were performed based on tracer data and on salinity data. The subsequent automatic calibration steps started each from their corresponding initial guess. Evidently, the parameter set from the salinity-based calibration was able to reproduce a realistic salinity gradient. The final parameter set from the tracer-based calibration, on the other hand, was more satisfactory in terms of convergence of the MCMC procedure (data not shown) than the one reported above, but severely underestimated the true salinity (Fig. 11). The question arises whether this strategy is viable to produce salinity gradients for future alternatives where no salinity data is available to verify the model output.

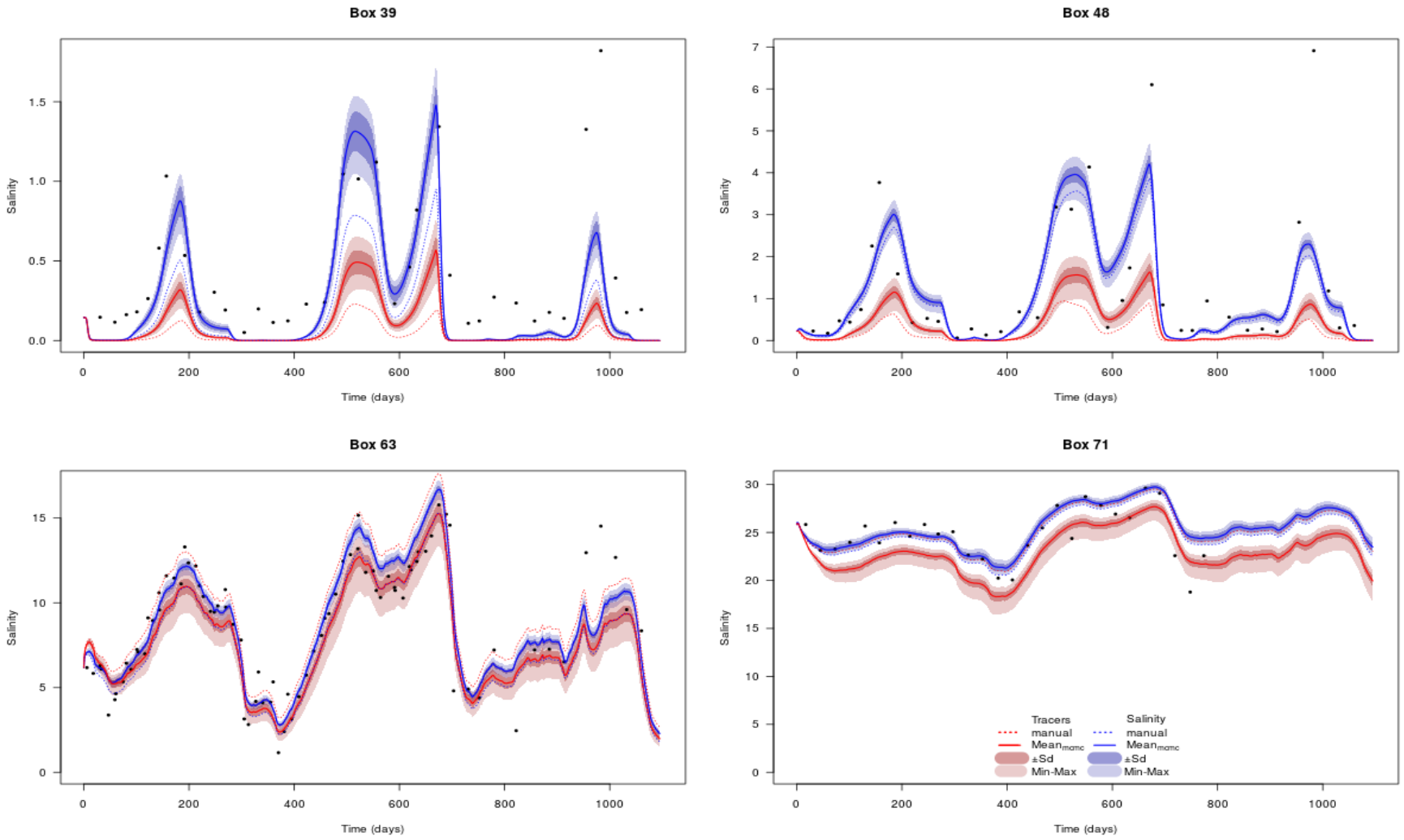

Fig. 11: Model-data comparison for the years 2010-2012 after calibrations to salinity and tracers. In this case, the automatic fitting routines each received their own initial parameter set after independent manual calibrations.

6. References

** IMDC/INBO/UA/WL, 2014. Modeling instruments for integrated plan Upper Sea Scheldt. Doc ref nr. I/NO/11448/14.165/DDP.*

* Soetaert K. and P.M.J. Herman (2009). A practical guide to ecological modeling. Springer, The Netherlands.

* Taverniers, ir. E.; Mostaert, dr. F. (2009). MONEOS - jaarboek monitoring WL 2008 : Overzicht monitoring hydrodynamiek en fysische parameters zoals door WL in 2008 in het Zeescheldebekken gemeten. Versie 4_0. WL Rapporten, Projectnr 833_07. Waterbouwkundig Laboratorium: Antwerpen, België

** WL2015_131_12, 2015. Tracer calculations for dispersion coefficients Scaldis 3D.*